

Testing Time Reversal Symmetry in Artificial Atoms

Frederico Brito,^{1,*} Francisco Rouxinol,² M. D. LaHaye,² and Amir O. Caldeira³

¹*Instituto de Física de São Carlos, Universidade de São Paulo, C.P. 369, São Carlos, SP,13560-970, Brazil*

²*Department of Physics, Syracuse University, Syracuse New York 13244-1130, USA*

³*Instituto de Física Gleb Wataghin, Universidade Estadual de Campinas-UNICAMP, 13083-859 Campinas, SP, Brazil*

Over the past several decades, a rich series of experiments has repeatedly verified the quantum nature of superconducting devices, leading some of these systems to be regarded as artificial atoms. In addition to their application in quantum information processing, these ‘atoms’ provide a test bed for studying quantum mechanics in macroscopic limits. Regarding the last point, we present here a feasible protocol for directly testing time reversal symmetry in a superconducting artificial atom. Time reversal symmetry is a fundamental property of quantum mechanics and is expected to hold if the dynamics of the artificial atom strictly follow the Schrödinger equation. However, this property has yet to be tested in any macroscopic quantum system. The test we propose is based on the verification of the microreversibility principle, providing a viable approach to verify quantum work fluctuation theorems - an outstanding challenge in quantum statistical mechanics. For this, we outline a procedure that utilizes the microreversibility test in conjunction with numerical emulations of Gibbs ensembles to verify these theorems over a large temperature range.

Few concepts in nature are so simple and yet as profound as those related to symmetry. Indeed, the beauty of its manifestations has led to the modern view that principles of symmetry dictate the forms of nature’s fundamental laws[1], embodying striking implications that range from conservation principles to the classification of elementary particles.

Time reversal symmetry (TRS) is a prominent example that underlies a large variety of phenomena. In many instances, the fundamental microscopic laws of nature are invariant under time reversal transformations. This invariance is at the heart of microscopic reversibility (microreversibility)[2], which itself is crucial to powerful concepts such as the principle of detailed balance[3], the fluctuation-dissipation theorem[4], and the Jarzynski equality[5], to name a few.

Yet TRS is not an exact symmetry of nature: in the very least, it is observed to be broken in elementary processes that involve the weak force[6, 7], and moreover, there is evidence to suggest that it must also be violated over a much broader range of conditions in order to account for the prevalence of matter over anti-matter in the universe[8, 9]. Manifestations of such violations potentially herald new phenomena and are thus the subject of extensive experimental investigations in both atomic and particle physics[9].

While considerable effort has been invested in the search for violations of TRS in the interactions of fundamental particles, experiments have not been conducted to investigate TRS in the physics of quantum systems at the macroscopic scale. Specifically, the question thus arises: Once one properly takes into account dissipative and decoherence effects, would TRS be observed in, say, a mesoscopic or even a macroscopic device? On the face of it, there is no reason to expect that it breaks down: we know the microscopic laws of quantum mechanics can be applied to at least some (properly prepared) macroscopic

systems. Nonetheless, if it does break down, this must reflect new physics, which could have potential connections to open questions like the nature of the quantum-classical divide[10, 11].

With these thoughts in mind, we delineate here a protocol for directly testing TRS at the macroscopic scale in an artificial atom that is based upon a superconducting quantum device (SQD). While similar types of SQDs are known for their use as qubits in the development of quantum computing architectures[12, 13], we propose to utilize an SQD as a multi-level artificial atom to test a specific manifestation of TRS, namely the principle of microreversibility.

Microreversibility and the artificial atom

Generally speaking, the principle of microreversibility states that for each state of motion that is accessible to a given system, there is an equally probable time-reversed state also accessible to it. In the context of quantum mechanics, it manifests in a simple relationship for the transition probabilities between any two states of a system whose Hamiltonian has undergone a time-dependent transformation[14], namely that

$$P_{n|m}[\lambda] = P_{m|n}[\tilde{\lambda}] \quad (1)$$

where $P_{n|m}(P_{m|n})$ is the probability for the system to make a transition to state $|m\rangle$ ($|n\rangle$) when it starts in state $|n\rangle$ ($|m\rangle$). Here λ represents the forward-in-time transformation of the system’s Hamiltonian and $\tilde{\lambda}$ represents the motion-reversed process (Fig. 1a).

Equation 1 is a fundamental and general result for non-dissipative quantum mechanical systems, deriving from the invariance of a system’s Hamiltonian under transformations by the anti-unitary time-reversal operator Θ [2, 14]. Thus it should hold true for all quantum systems in which TRS is maintained. Naively, one would expect this to include macroscopic systems for which the laws of

quantum mechanics have been shown to apply, such as mechanical quantum systems[15, 16] and superconducting cavities, circuits and devices[12, 13, 17–19]. However, a direct test of TRS in these systems has yet to be performed. As we show now, it should be technologically feasible to perform a test of microreversibility, and hence TRS, via Eq. 1, in an artificial atom based upon an SQD.

The SQD here is a Cooper-Pair box (CPB), which in our proposal consists of a nanofabricated superconducting island (or box) that is formed by a pair of Josephson junctions in a DC SQUID configuration (Fig. 1b). The system is well-characterized by the following Hamiltonian[20]

$$H = 4E_C \sum_n (n - n_g)^2 |n\rangle \langle n| - \sum_n \left[\frac{\mathcal{E}_J(\Phi)}{2} |n\rangle \langle n+1| + \frac{\mathcal{E}_J^*(\Phi)}{2} |n+1\rangle \langle n| \right]. \quad (2)$$

The first term on the right-hand side of Eq. 2 represents the electrostatic energy of the CPB for a given charge state n (a discrete index labelling the number of Cooper-pairs on the island) and continuous polarization charge n_g on a nearby electrode; the pre-factor E_C is the total charging energy of the CPB. The second term on the right in Eq. 2 represents the mixing of charge states due to the Josephson coupling of each junction. Here $\mathcal{E}_J(\Phi) \equiv E_{J\Sigma} \left\{ \cos\left(\pi \frac{\Phi}{\Phi_0}\right) + i\alpha \sin\left(\pi \frac{\Phi}{\Phi_0}\right) \right\}$ is the total Josephson energy of the two junctions; observe that $|\mathcal{E}_J(\Phi)|$ is periodic in applied magnetic flux Φ with a period of one flux quantum Φ_0 . To account for asymmetry between the junctions, we define the parameter $\alpha \equiv (E_{J1} - E_{J2})/E_{J\Sigma}$, where $E_{J\Sigma} \equiv E_{J1} + E_{J2}$ is the sum of the individual junction Josephson energies E_{J1} and E_{J2} .

It is important to note that numerous experiments over the past 15 years have shown that the two parameters Φ and n_g in Eq. 2 can be tuned *in situ* for experimental implementation of unitary operations with the CPB [12, 13]. The proposal we put forth for testing Eq. 1 exploits this coherent control. Specifically, it relies upon the adjustment of Φ and n_g to modify the characteristics of the CPB's energy eigenstates. To understand how this might work, observe that, when Φ is adjusted so that $|\mathcal{E}_J|$ is relatively small (i.e $\beta \equiv |\mathcal{E}_J|/(4E_C) \ll 1$), and n_g is adjusted near an integer, the eigenstates of the system are essentially the charge states $|n\rangle$. On the other hand, if $\beta \gtrsim 1$, or n_g is near a half-integer, then the eigenstates are no longer well-defined charge states, but instead are weighted superpositions of multiple values of $|n\rangle$. Thus, through the rapid tuning of Φ and n_g , the CPB can be forced to undergo unitary evolution between various superpositions of charge states. Through repeated projective measurements of the CPB's charge state before (n) and after (m) identical forcing protocols, the transition probabilities $P_{n|m}$ between any given pair of charge states

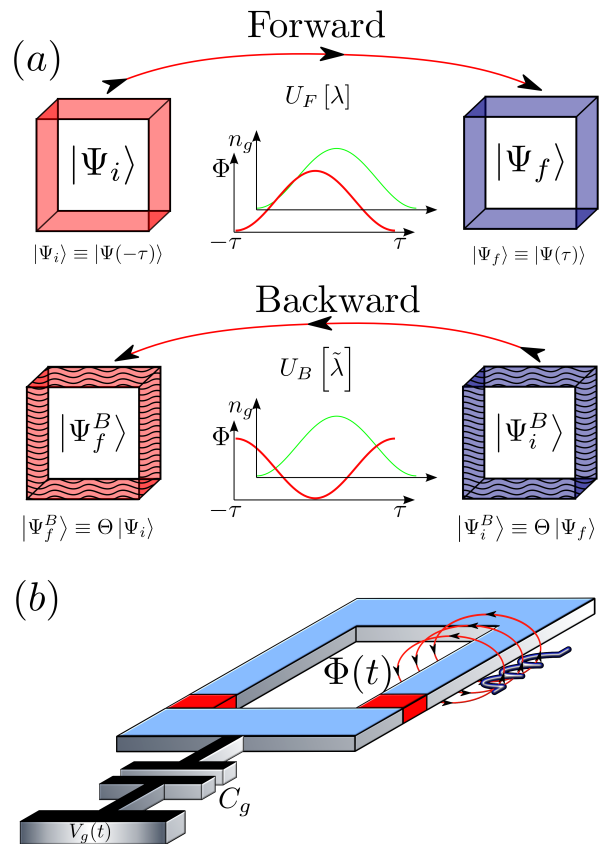


FIG. 1. Schematics of TRS for driven (nonautonomous) quantum systems and the Artificial Atom. **a**, While the unitary time evolution of the forward-in-time protocol takes the initial state $|\Psi_i\rangle$ to the evolved state $|\Psi_f\rangle = U_F[\lambda]|\Psi_i\rangle$, the motion reversed state follows the dynamics $|\Psi_f^B\rangle \equiv \Theta|\Psi_i\rangle = U_B[\tilde{\lambda}]\Theta|\Psi_f\rangle$, where Θ represents the time reversal operator. In this generalization, $\Phi(t)$ and $n_g(t)$ represent time-dependent parameters in the system's Hamiltonian which are tuned to change the state of the system. If a system parameter depends upon an applied magnetic field, then the field must be inverted to move from the Forward to the Backward protocol as shown schematically with $\Phi(t)$. **b**, SQD based upon a CPB, used to implement the artificial atom in our protocol. The system dynamics can be controlled by adjusting the magnetic flux $\Phi(t)$ through the loop and the charge $n_g(t) = C_g V_g(t)/2e$ on a nearby electrode, where C_g is the capacitance of the CPB to the electrode and $V_g(t)$ is an externally controlled voltage. The device features two Josephson junctions (red boxes), arranged in parallel, interrupting the loop. The physical dimensions assumed here are such that the geometrical inductance is negligible compared to the Josephson inductances, leading to the Hamiltonian Eq. (2), where: $E_C/\hbar = 2\pi \times 3\text{GHz}$, $E_{J\Sigma}/\hbar = 2\pi \times 10\text{GHz}$, and $\alpha = 0.05$.

$|n\rangle$ and $|m\rangle$ in the spectral decompositions of the initial and final states can be constructed.

Forward and backward protocols

Our specific proposal to test Eq. 1 is outlined in Figs.

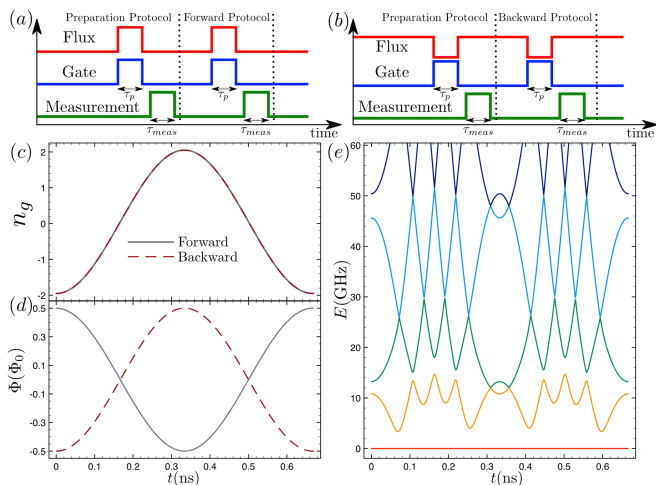


FIG. 2. **Protocol scheme and system's eigenenergies versus time.** **a-b**, Outline of the Forward and Backward protocols. The first step, the Preparation Protocol, is used to construct an initial ensemble of several charge states. After the first measurement is performed, a driving protocol is used to implement a forward and backward-in-time evolution, which is followed by another charge measurement. After many runs, the transition probabilities between the allowed initial and final states can be constructed. **c-d**, The time forward (solid line) and backward (dashed line) drive protocols for the gate charge n_g and flux Φ . In order to maintain the time reversal symmetry, the sign of the magnetic field must be inverted. **e**, The eigenenergies of the CPB as function of time during the driving protocol (the ground state energy is set zero). It is worth noticing the presence of several avoided level crossings, where Landau-Zener transitions are induced. The eigenenergies are calculated for the same parameters stated in Fig. 1.

2a-d. It involves the application of two separate protocols to the CPB to measure $P_{n|m}[\lambda]$ and $P_{m|n}[\tilde{\lambda}]$, which we refer to as the forward (λ) protocol and the backward ($\tilde{\lambda}$) protocol respectively. For process λ , the CPB is taken through the following sequence of steps: (1) First with the CPB initialized in its ground state, a pulse sequence consisting of the simultaneous application of time-varying signals $n_g(t)$ and $\Phi(t)$ (Figs. 2c-d) is applied to CPB, causing it to repeatedly pass through avoided-level crossings in its energy spectrum (Fig. 2e). At each such crossing, the CPB can undergo a Landau-Zener transition[21, 22] between the adjacent states involved in the crossing, which leaves it in a superposition of those two states. For the parameters considered here, after traversing the multiple crossings shown in Fig. 2e, the CPB state should be in a superposition of as many as 5 charge states. (2) Immediately after the initial superposition state is prepared, a projective measurement of the CPB's charge is made and recorded as state n . We refer to those steps as the Preparation Protocol (Figs. 2a-b), since they provide an effective way for preparing

an initial ensemble of charge states which can be used for measuring $P_{n|m}$ -in our case, its composition is given in (Fig. 3a). (3) Next, after the collapse to the charge state $|n\rangle$, a second pulse sequence identical to the sequence in step (1) is applied, again preparing the CPB in a superposition of charge states. (4) Finally, a second projective measurement of the CPB charge state is made and recorded as m . After step (4), the CPB is allowed sufficient time to relax back to its ground state, after which time λ is repeated. In this manner, the transitions probabilities $P_{n|m}[\lambda]$ can be constructed. Figure 3b illustrates a histogram of $P_{n|m}[\lambda]$ for this process calculated with numerical simulations using Eq. 2 and the pulse sequences in Figs. 2c-d (See Methods section).

To implement the time-reversed process $\tilde{\lambda}$ and construct the corresponding transition probabilities $P_{m|n}[\tilde{\lambda}]$, the same general procedure as outlined in the previous paragraph is followed. However, it is necessary to change two physical quantities for the time-reversed process: First, the sign of the magnetic flux applied to the CPB must be reversed to account for the reversal of momentum of the magnetic field's source charges. Observe that such inversion leads to $\mathcal{E}_J(-\Phi) = \mathcal{E}_J^*(\Phi)$. Second, one should also invert the sign of the appropriate canonical variable of the CPB during $\tilde{\lambda}$, which in this case turns out to be the effective phase difference φ across the CPB's Josephson junctions. This step is necessary to preserve the time-reversal invariance of the canonical charge-phase commutation relations, since charge is considered an invariant under TRS. In our particular case, inverting the sign of φ has the effect of conjugating \mathcal{E}_J . Therefore, as one would expect, applying those two changes leaves the system Hamiltonian invariant. In addition, since we have a time-dependent Hamiltonian (nonautonomous system)[14], we also have to revert the forcing protocol applied to the system, i.e., $|\Phi(t)\rangle \rightarrow |\Phi(-t)\rangle$ and $n_g(t) \rightarrow n_g(-t)$. With these changes, numerical simulations of the backward protocol indeed predict that Eq. 1 should hold (Fig. 3c) (See Methods section).

Conditions for unitarity and the measurement protocol

To claim a true test of TRS through verification of microreversibility (Eq. 1), it is essential that the CPB's time evolution be predominantly unitary during the λ and $\tilde{\lambda}$ protocols. This requires that the protocols be implemented on a time scale τ_p that is much faster than any environmental effects. By applying the methodology introduced by Burkard-Koch-DiVincenzo[23], one finds that the figure of merit for quantifying such effects in our protocol is the relaxation time T_1 . It can be shown that the decoherence time T_2 is determined by T_1 ($T_2 \sim 2T_1$), except for the regime $\beta \ll 1$, which corresponds to a tiny window of $\sim 0.2ns$ in the protocol, during which

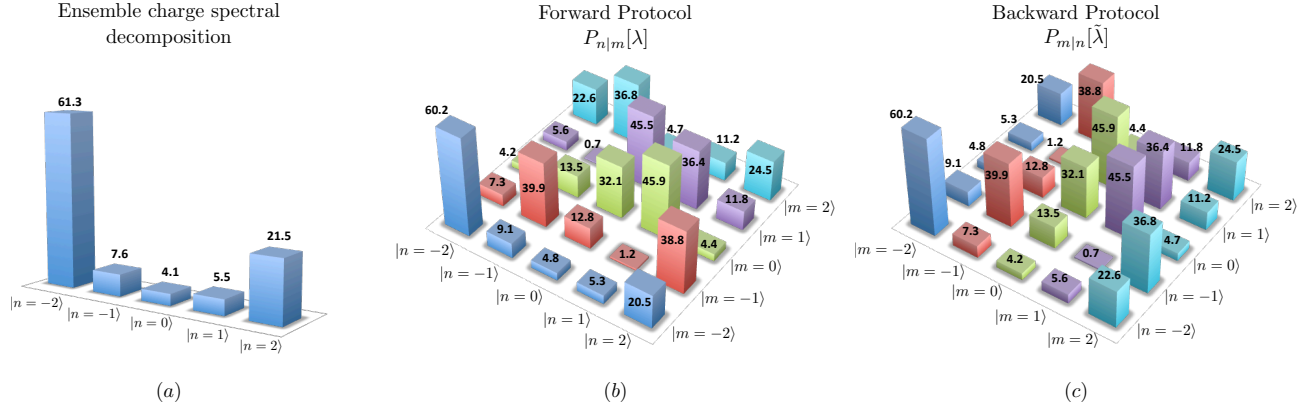


FIG. 3. **Compiled probability distributions for preparation, forward and backward protocols.** **a**, The charge ensemble distribution (%) prepared after starting the system in the ground state and performing the Preparation Protocol. For the parameters considered here, the spectral decomposition obtained is predominantly ($> 99.9\%$) comprised of charge states $\{-2, -1, 0, 1, 2\}$. **b(c)**, The probability transitions $P_{n|m}$ (%) between the initial $|n\rangle$ and final $|m\rangle$ charge states determined for the Forward λ (Backward $\tilde{\lambda}$) protocol. The leakage probability of leaving the charge subspace $\{-2, -1, 0, 1, 2\}$ is determined to be $\lesssim 0.1\%$. Observe that microreversibility demands comparing columns of (b) with rows of (c). The spectral decomposition and transition probabilities are calculated for the same parameters stated in Fig. 1.

$T_2 \sim 0.02T_1$ (See Methods section). Thus, even for a modest T_1 of 50ns, which is readily achievable with current technology[24], the designed protocol with $\tau_p \sim 1ns$ (Figs. 2a-b) should provide a satisfactory unitary evolution.

It is also important that the projective charge measurements are made within a time-scale $\tau_{meas} \ll T_1$. That T_1 sets the relevant time-scale can be understood by realizing that decoherence effects becomes innocuous if one chooses projective measurements in the eigenenergy basis, since such effects would not lead to changes in the system state eigenenergy spectral decomposition. Notice from Fig. 2d that our protocol complies with this case: at the end of a protocol, when a projective measurement of charge is made, the CPB is biased so that the charge states are quasi-eigenenergy states of the system (i.e. $\beta \ll 1$). Hence these measurements should also each be performed on a time scale $\tau_{meas} \lesssim 10ns$. A natural and viable possibility for performing such high-speed, high-sensitivity charge measurements would be to use a superconducting single electron transistor (SSET)[25–27]. When operated in RF mode, SSETs can have bandwidth in excess of 100 MHz [25] and charge detection sensitivity approaching the limit allowed by quantum mechanics [26, 27]. Indeed, assuming the detection sensitivity achieved in Ref. [26], it should be possible to resolve the CPB’s charge state with an error of $\sim 0.5\%$ in a time scale of $t_{meas} \sim 20ns$ (See Methods section).

Gibbs ensemble emulation and quantum work fluctuation relation

In addition to testing TRS in new macroscopic quan-

tum limits, the investigations that we have outlined here would have implications for at least one contemporary avenue of investigation: quantum work fluctuation theorems. Indeed, to derive these theorems, it is sufficient to make two hypotheses: the microreversibility principle and the assumption that the system is initially in thermal equilibrium at temperature T (a Gibbsian distribution)[14].

One paradigm of such work fluctuation relations is the quantum Bochkov-Kuzovlev equality[28]

$$\langle e^{-W/k_B T} \rangle = 1 \quad (3)$$

which states that the work distribution of any driving protocol applied to a system initially in thermal equilibrium at temperature T is a random quantity, whose expected value does not depend on the details of either the system or the driving protocol. To test Eq. 3 using an SQD would require running an experiment at very low temperature ($T \sim 30mK$), in which case the SQD’s initial thermal state is predominantly the population of the system ground state. Unfortunately this leads to very poor statistics for Eq. 3. In principle, this problem could be solved by just increasing the system temperature, but in order to obtain a Gibbsian distribution comprised of a reasonable number of states, e.g., 5 states, one should perform the experiment at $T \sim 1K$, which certainly would destroy the unitary evolution required for microreversibility to hold.

Here, we envision a solution to this problem by constructing a thermal state out of the initial charge ensemble obtained in the preparation protocol, which we name an emulation of an initial Gibbs ensemble. The procedure consists of randomly selecting the outcomes of

the first measurement following the probability rule imposed by the Boltzmann weight $\exp(-H/k_B T)$. If the number of experimental events is sufficiently large, such distribution can be obtained for a given temperature T . Indeed, as Table I shows, for 10^6 events, one can emulate a Gibbs ensemble comprised of those 5 states for temperatures above $1K$, and verify with a small statistical error the quantum Bochkov-Kuzovlev equality (See Methods section).

TABLE I. Emulation for 10^6 Events

Temperature (K)	$1 - \langle e^{-W/k_B T} \rangle$
1	$(-0.4 \pm 5.8) \times 10^{-2}$
10	$(-2.7 \pm 7.9) \times 10^{-4}$
20	$(-2.1 \pm 4.2) \times 10^{-4}$
30	$(-0.6 \pm 3.0) \times 10^{-4}$
40	$(-0.1 \pm 2.2) \times 10^{-4}$
50	$(-0.3 \pm 1.7) \times 10^{-4}$

In the present paper we have created a protocol for the preparation, time evolution and measurement of the quantum state of an SQD in order to test TRS in a new regime using state-of-the-art technology and techniques. Our numerical simulations show that the repeated application of this protocol to the SQD would enable verification of the microreversibility principle. An immediate application of this result is the confirmation of the fluctuation relations for which microreversibility and an initial Gibbsian distribution are necessary conditions. Using the results of our simulations, we show how to fulfil this latter requirement by emulating a possible initial equilibrium state of the system, which together with microreversibility allowed us to numerically verify one of the possible forms of the fluctuation relations, namely, the Bochkov-Kuzovlev equality.

Although one could argue that our results are formally expected, their experimental observation would be of utmost importance and the reason is threefold. Firstly, it would provide the first direct test of the microreversibility of transitions between the states of a macroscopic quantum system. Secondly, operating on a single system, one would be able to emulate the results one would have obtained starting from an ensemble of systems in thermodynamic equilibrium, and consequently confirm the quantum fluctuation relations without actually raising the temperature of the system. Finally, if microreversibility is indeed observed in this kind of system it may constitute additional possible evidence to rule out alternative theories for quantum mechanics such as the dynamical reduction models[29]. Since the latter assumes a non-linear stochastic dynamics to macroscopic observables of a given system, it cannot be time reversal invariant, contrary to our predictions.

Methods

Numerical simulations

The system's state time evolution was determined through numerical simulations of the unitary time-ordered evolution operator due to the Hamiltonian Eq. 2. The calculation was performed taking into account an $N = 51$ charge dimensional Hilbert space. Considering the time discretization procedure and the Hilbert space truncation, we estimated a maximum relative error of $\sim 0.05\%$ for the probabilities quoted in the main text. The specific flux and charge pulses used in our protocol read: $\Phi(t) = (\Phi_0/2) \cos(2\pi \times \frac{3}{2} \times t)$ and $n_g(t) = 0.05 - 2 \cos(2\pi \times \frac{3}{2} \times t)$, with time in unit of nanoseconds.

Decoherence and relaxation rates for the CPB

The methodology introduced by Burkard-Koch-DiVincenzo[23] allows one to use circuit theory for describing the dissipative elements of the circuit with a bath of oscillators model, from which it is possible to calculate the dissipative effects for multilevel superconducting devices. From this modelling, the system-bath coupling derived is a functional of the charge number operator n . Therefore, it will only connect the system energy eigenstates that have at least one charge state in common in their spectral decomposition. For the physical CPB parameters and the flux and charge protocols considered in our proposal, we found that only neighbouring eigenstates share one charge state in their spectral decomposition. Thus, with a good approximation, the dissipative process can be viewed as a sequence of multiple processes involving only two eigenstates. Under this perspective, one can obtain the relaxation (T_1) and decoherence (T_2) times concerning those two levels. In the Born-Markov approximation, the relation between T_1 and the pure dephasing T_ϕ is found to be

$$\frac{T_\phi}{T_1} \sim \frac{4 |\langle e_k | n | e_{k+1} \rangle|^2}{|\langle e_k | n | e_k \rangle - \langle e_{k+1} | n | e_{k+1} \rangle|^2} \frac{e_{k+1} - e_k}{2k_B T} \coth \frac{e_{k+1} - e_k}{2k_B T},$$

where e_k is the instantaneous value of the eigenenergy state k , and $T_2^{-1} = T_1^{-1}/2 + T_\phi^{-1}$. Performing the calculation of the matrix elements above for each time instant of our protocol, we found that the decoherence time T_2 is determined by T_1 , i.e., $T_\phi \gg T_1$, except for the regime $\beta \ll 1$, during which $T_2 \sim 0.02T_1$. Observe that for $\beta \ll 1$ (the SQD charge regime), the charge operator n almost commutes with the system Hamiltonian, which explains why T_1 becomes the longest time scale here.

Estimate of the CPB measurement uncertainty

To estimate the CPB charge-state measurement uncertainty, we first assume that the CPB is probed using an SSET that is coupled to the CPB through a capacitance C_C . It is further assumed that the SSET charge sensitivity S_Q is dominated by the noise of the pre-amplifier used to read-out the SSET. In this case, for each Cooper-pair number state N , the inferred charge (Q_C) on C_C will have a Gaussian distribution $p_N(Q_C)$ with R.M.S. of $\sigma_Q = \sqrt{(S_Q/\tau_{meas})}$, where τ_{meas} is the measurement time. We then define the measurement uncertainty through the use of the Kolmogorov (trace) distance [30], which is given by $D(p_N(Q_C), p_{(N+1)}(Q_C)) = (1/2) \int |p_N(Q_C) - p_{(N+1)}(Q_C)| dQ_C$. The probability to correctly identify from which of two adjacent probability distributions $p_N(Q_C)$ and $p_{(N+1)}(Q_C)$ an outcome of a measurement Q_C comes is thus given by $P_D = (1 + D)/2$. For example, using $S_Q^{1/2} = 1.7\mu\text{e}/\sqrt{\text{Hz}}$, which was achieved in [26], a measurement time $\tau_{meas} = 20\text{ns}$, and realistic parameters for the total capacitance of the CPB island $C_\Sigma = 6.5\text{fF}$ (corresponding to $E_C/\hbar = 2\pi \times 3\text{GHz}$) and $C_C = 0.20\text{fF}$, we find $P_D = 99.5\%$, corresponding to a measurement uncertainty of 0.5%.

Quantum work and the Gibbs ensemble generator

The quantum Bochkov-Kuzovlev equality Eq. 3 is derived[28] considering the *exclusive viewpoint* for the definition of quantum work. Such definition considers that the quantum work performed in a specific process λ is determined as the difference of the outcomes of the eigenenergy measurements of the unperturbed system Hamiltonian done at the initial and final process times. In our case,

the Hamiltonian Eq. 2 can be viewed as $H(t) = H_0 + H_p[\lambda(t)]$, where the unperturbed Hamiltonian H_0 is set as $H(t = 0)$, and the force-dependent Hamiltonian perturbation $H_p[\lambda(t)]$ is given by $H(t) - H_0$.

The Gibbs ensemble emulation is constructed using a standard pseudorandom routine to select the states out of the initial ensemble obtained from the preparation protocol. The pseudorandom choice is weighted by the Boltzmann weight for a given temperature T .

Acknowledgements

FB and AOC are supported by Instituto Nacional de Ciência e Tecnologia - Informação Quântica (INCT-IQ) and by Fundação de Amparo à Pesquisa do Estado de São Paulo (FAPESP) under grant number 2012/51589-1. MDL and FR acknowledge support for this work provided by the National Science Foundation under Grant No. DMR-1056423 and Grant No. DMR-1312421.

Author contributions

All authors contributed equally to this work.

* fbb@ifsc.usp.br

- [1] Gross, D. J. The role of symmetry in fundamental physics. *Proc. Nat. Acad. Sci.* **93**, 14256 (1996).
- [2] Messiah, A. *Quantum Mechanics* (Dover Publications, Mineola, 1999).
- [3] Reichl, L. E. *A Modern Course In Statistical Physics*, second edition (John Wiley & Sons, New York, 1998).
- [4] Callen, H. B. & Welton, T. A. Irreversibility and generalized noise. *Phys. Rev. E* **83**, 34 (1951).
- [5] Jarzynski, C. Nonequilibrium equality for free energy differences. *Phys. Rev. Lett.* **78**, 2690 (1997).
- [6] Lees, J. P. *et al.* Observation of Time-Reversal Violation in the B^0 Meson System. *Phys. Rev. Lett.* **109**, 211801 (2012).
- [7] Bernabéu, J. Time reversal violation for entangled neutral mesons. *Journal of Physics: Conference Series* **447**, 012005 (2013).
- [8] Sakharov, A. D. Violation of CP invariance, C asymmetry and baryon asymmetry of universe. *JETP Letters* **5**, 24 (1967).
- [9] Henley, E.M. Time Reversal Symmetry. *Int. J. Mod. Phys. E* **22**, 1330010 (2013).
- [10] Leggett, A. J. Testing the limits of quantum mechanics: motivation, state of play, prospects. *J. Phys.: Condens. Matter* **14**, R415 (2002).
- [11] Ball, P. *Nature* **453**, 22 (2008).
- [12] Clarke, J. & Wilhelm, F. K. Superconducting quantum bits. *Nature* **453**, 7198 (2008).
- [13] Devoret, M.H. & Shoelkopf, R.J. Superconducting circuits for quantum information: An outlook. *Science* **339**, 1169 (2013).
- [14] Campisi, M., Hänggi, P. & Talkner, P. Quantum fluctuation relations: Foundations and applications. *Rev. Mod. Phys.* **83**, 771 (2011).
- [15] O'Connell, A. D. *et al.* Quantum ground state and single-phonon control of a mechanical resonator. *Nature* **464**, 697 (2010).
- [16] Palomaki, T. A., Teufel, J. D., Simmonds, R. W. & Lehnert, K. W. Entangling mechanical motion with microwave fields. *Science* **342**, 710 (2013).
- [17] Raimond, J.M., Brune, M. & Haroche, S. Colloquium: Manipulating quantum entanglement with atoms and photons in a cavity. *Rev. Mod. Phys.* **73**, 565 (2001).
- [18] Mooij, J. E. *Nat. Phys.* **6**, 401 (2010).
- [19] Houck, A.A., Türeci, H.E. & Koch, J. On-chip quantum simulation with superconducting circuits. *Nat. Phys.* **8**, 292 (2012).
- [20] Makhlin, Y., Schön, G. & Shnirman, A. Quantum-state engineering with Josephson-junction devices. *Rev. Mod. Phys.* **73**, 357 (2001).
- [21] Zener, C. Non-Adiabatic Crossing of Energy Levels. *Proc. R. Soc. Lond. A* **137**, 696 (1932).
- [22] Shevchenko, S.N., Ashhab, S., & Nori, F. Landau-Zener-Stückelberg interferometry. *Phys. Rep.* **492**, 1 (2010).
- [23] Burkard, G., Koch, R. H. & DiVincenzo, D. P. Multilevel quantum description of decoherence in superconducting qubits. *Phys. Rev. B* **69**, 064503 (2004).
- [24] Wallraff, A. *et al.* Strong coupling of a single photon to a superconducting qubit using circuit quantum electrodynamics. *Nature* **431**, 162 (2004).
- [25] Schoelkopf, R.J. *et al.* The radio-frequency single-electron transistor(RF-SET): A fast and ultrasensitive electrometer. *Science* **280**, 1238 (1998).
- [26] Xue, W..W *et al.* Measurement of the quantum noise of a single-electron transistor near the quantum limit. *Nat. Phys.* **5**, 660 (2009).
- [27] Clerk, A.A., Girvin, S.N., Ngyuen, A.K. & Stone, A.D. Resonant Cooper-pair tunneling: Quantum noise and measurement characteristics. *Phys. Rev. Lett.* **89**, 176804 (2002).
- [28] Campisi, M., Talkner, P. & Hänggi, P. Quantum Bochkov-Kuzovlev work fluctuation theorems. *Phil. Trans. R. Soc. A* **369**, 291 (2011).
- [29] Bassi, A. & Ghirardi, G. Dynamical reduction models. *Phys. Rept.* **379**, 257 (2003).
- [30] Nielsen, A. C. & Chuang, I. L. *Quantum Computation and Quantum Information* (Cambridge University Press, Cambridge, 2000).